

## Characterization and reactivity of group III oxides supported on niobium oxide

A.L. Petre<sup>a</sup>, J.A. Perdigón-Melón<sup>a</sup>, A. Gervasini<sup>b</sup>, A. Auroux<sup>a,\*</sup>

<sup>a</sup> *Institut de Recherches sur la Catalyse, CNRS, 2 Avenue Albert Einstein, 69626 Villeurbanne Cedex, France*

<sup>b</sup> *Dipartimento di Chimica Fisica ed Elettrochimica, Università di Milano, Via Golgi 19, 20133 Milano, Italy*

### Abstract

A series of group III oxides supported on niobia were prepared by incipient wetness impregnation. The bulk and surface composition of the samples as well as their structural and textural features were determined by chemical analysis, nitrogen adsorption, XRD, TG-DSC and XPS measurements. Acid/base properties were studied by adsorption microcalorimetry using ammonia and sulfur dioxide as probe molecules. The catalytic performances in non-oxidative dehydrogenation of propane have been studied and related to the physico-chemical characteristics of the samples.

© 2002 Elsevier Science B.V. All rights reserved.

**Keywords:** Niobia supported Al–Ga–In-oxides; Acidity; Propane dehydrogenation

### 1. Introduction

Hydroxyl groups play an important role in the surface properties and especially the acid–base behavior of Nb<sub>2</sub>O<sub>5</sub>, because they can either be retained on the surface of Nb<sub>2</sub>O<sub>5</sub> as Brønsted acid sites (responsible e.g. for the well-known high acidity of niobic acid, Nb<sub>2</sub>O<sub>5</sub>·*n*H<sub>2</sub>O) or form Lewis acid sites by detachment in pairs upon high temperature treatment. The special properties (redox properties, photosensitivity, acidity and catalytic behavior) of compounds containing niobium, such as niobium phosphate, niobia mixed oxides and niobium layer compounds are responsible for the strong motivation to understand and use for catalytic purposes the advantages of these materials [1,2]. Also, niobia is a typical strong metal-support interaction (SMSI) oxide [3] and well-known to exhibit a

pronounced effect as a support for metal and metal oxide catalysts.

Until now, research has focused mostly on the investigation of superficial properties and catalytic performance of supported niobium oxide catalysts prepared by various methods, rather than on metal oxides deposited on niobia supports.

For example, the surface acidic properties of alumina-supported niobia prepared by chemical vapor deposition and hydrolysis of niobium pentachloride have been studied by TPD of ammonia and infrared spectroscopy of adsorbed pyridine [4]. The catalysts with the lowest niobium content displayed a higher density of acid sites than the alumina support, and the acidity decreased with an increase in the niobium content. Brønsted acid sites were identified only on the surface of a pure niobium oxide sample [4].

In other studies [5–7] Lewis acid sites have been found in supported niobium oxide systems prepared by incipient wetness impregnation of silica, magnesia, alumina, titania and zirconia, while Brønsted acid sites

\* Corresponding author. Tel.: +33-472-445300;  
fax: +33-472-445399.  
E-mail address: auroux@catalyse.univ-lyon1.fr (A. Auroux).

were only detected for niobia supported on alumina and silica, in amounts increasing with the loading of niobia.

On the other hand, gallium oxide and indium oxide are well-known and frequently studied as semiconductor materials, used for many applications such as sensor devices for the detection of  $\text{NO}_x$ ,  $\text{O}_2$ ,  $\text{H}_2\text{O}$ ,  $\text{CO}$  [8,9]. Recently, certain group III oxides ( $\text{Al}_2\text{O}_3$ ,  $\text{Ga}_2\text{O}_3$ ,  $\text{In}_2\text{O}_3$ ) have attracted much interest as catalysts for selective catalytic reduction of  $\text{NO}_x$  by hydrocarbons in the presence of excess oxygen [10,11] and for the dehydrogenation or aromatization of light alkanes [12]. It was proved that the catalytic performances in both processes were highly affected by the support effect, hence the importance of the choice of support in the development of highly efficient catalysts.

Therefore, the acid–base properties of niobia supports may be affected by the deposition of Al, Ga, or In amphoteric oxides. The good catalytic results obtained in non-oxidative dehydrogenation of light alkanes using bulk  $\text{Ga}_2\text{O}_3$ , supported gallium oxide catalysts and zeolites containing gallium and indium, as well as those of niobia in oxidative conditions, provided determinant motivation to examine the catalytic properties of group III oxides supported on niobia [12–15].

It is expected that, by studying the changes in the acid–base properties, one can gain useful information on the guest metal oxides, including their dispersion and loading on the niobia catalyst surface, thus allowing one to enhance the catalytic properties.

In the present study, the structural features, acid/base and catalytic properties in non-oxidative dehydrogenation of propane of alumina, gallia and india supported on niobium oxide were investigated in order to determine the specific effect of the deposited metal oxide as well as the quality of dispersion on the niobia support.

## 2. Experimental

A series of group III (Al, Ga and In) oxides supported on niobium oxide with a loading close to the theoretical monolayer (called respectively Al/Nb, Ga/Nb and In/Nb) has been synthesized. The samples were prepared by incipient wetness impregnation of

niobium oxide (obtained by dehydration of commercial niobium pentoxide hydrate, niobia HY-340, from Companhia Brasileira de Metalurgia e Mineração Brasil for 8 h at 523 K in  $\text{O}_2$  flow) with the appropriate amounts of the corresponding nitrate solutions,  $\text{In}(\text{NO}_3)_3 \cdot 5\text{H}_2\text{O}$  from Aldrich Chemical Company purity 99.9%,  $\text{Ga}(\text{NO}_3)_3 \cdot 10\text{H}_2\text{O}$  from Strem Chemicals purity 99.99% and  $\text{Al}(\text{NO}_3)_3 \cdot 9\text{H}_2\text{O}$  from Fluka purity 99%. After impregnation the samples were dried at 393 K for 12 h and calcined at 773 K for 12 h in oxygen flow. A sample of niobium oxide dehydrated in the same conditions was used as reference.

The concentrations of the supported metal oxides were determined by AES-ICP in a Spectroflame-ICP instrument. Surface areas were determined by the BET method from the adsorption of nitrogen at 77 K. The crystallographic structure was examined by X-ray diffraction in a Bruker (Siemens) D5005 apparatus ( $\text{Cu K}\alpha$  radiation, 0.154 nm). The atomic ratios between metal of supported oxide and niobium were determined by XPS performed at room temperature with an SSI 301 spectrometer. A differential scanning calorimeter (Setaram TG-DSC-111) was used in order to determine the temperature of niobia phase transition. The experiments were carried out in oxygen flow, using a heating rate of  $2 \text{ K min}^{-1}$  up to 923 K.

Adsorption microcalorimetry is arguably the most direct method for describing in detail the features of surface sites simultaneously from a quantitative and from an energetic viewpoint. The structural and/or chemical heterogeneities of the sample surfaces were pictured by adsorbing suitable probe molecules and measuring the heats evolved at increasing coverages. Ammonia and sulfur dioxide were chosen to probe the acidity and basicity of the catalysts respectively. The measurements were carried out isothermally at 353 K (or other temperatures when explicitly indicated) in a heat flow calorimeter (Setaram C80) coupled with a standard volumetric apparatus. Successive doses of gas were sent to the sample until a final pressure of 0.5 Torr was obtained. The sample was then evacuated for 30 min at the same temperature in order to remove the amount physically adsorbed, and a second adsorption was performed. The quantity adsorbed at 0.2 Torr in the first adsorption will be called  $V_T$ . The difference between the amounts adsorbed in the first and second adsorptions at 0.2 Torr is the irreversibly chemisorbed amount ( $V_{\text{irr}}$ ). The samples were

pretreated at 673 K in vacuum overnight before the measurements.

All the samples were tested in the reaction of non-oxidative dehydrogenation of propane. The catalytic tests were performed in a tubular quartz flow microreactor using a catalyst charge of 0.5 g, without dilution, supported by quartz wool. The samples were activated by heating at 673 K under air flow overnight and then flushed with nitrogen for 30 min. The gas mixture was  $C_3H_8:N_2 = 1:4$  with a total flow rate of  $2.5\text{ l h}^{-1}$ . The runs were performed in the range 673–873 K. Between two successive runs the sample was flushed with air for 15 min. The reaction products were analyzed in an FID chromatographic system with a packed column (Unibead 3S). The reactant conversion and the selectivity towards propene were monitored as functions of temperature.

### 3. Results and discussion

The surface area, the metal oxide loading expressed in weight percent and the atomic ratio between metal of supported group III oxide and niobium are summarized in Table 1 for all the samples.

The theoretical geometric monolayer loadings [16] and the experimental loadings determined by chemical analysis are very similar, the experimental values being slightly lower in all cases. A more precise image of the real concentration of the guest oxide on the catalyst surface was obtained by means of XPS measurements. Comparing the M (M = Al, Ga, In)/Nb atomic ratios calculated from AES-ICP and determined from XPS (Table 1), it can be concluded that dispersions decrease as we descend in the group: the best dispersion has been obtained for the supported alumina sample, gallium and indium oxide being less dispersed on the niobia surface. The fact that the M/Nb ratios obtained

by XPS were higher than those obtained by chemical analysis shows that aluminum, gallium and indium are indeed located at the surface of the  $Nb_2O_5$  support, whereas the two ratios would be identical in the case of a solid solution.

No periodic behavior can be established for the variation of catalyst surface areas. Al/Nb presents a slightly higher surface area than the niobia support, while Ga/Nb and In/Nb display surface areas very similar to each other and lower than that of  $Nb_2O_5$ . This suggests that the formation of  $InO_x$  and  $GaO_x$  aggregates on the support surface, which could be located on interparticle voids or in the pores of  $Nb_2O_5$ , causing the abrupt decrease of surface area of Ga/Nb and In/Nb compared with that of the  $Nb_2O_5$  support. Conversely, the preservation of the high surface area of the Al/Nb sample reflects the good dispersion of  $AlO_x$  species on the  $Nb_2O_5$  support, which contribute to increase the surface area of the sample with respect to the bare support.

The XRD spectra of samples as synthesized and after TG-DSC experiments are represented in Fig. 1(a) and (b), respectively. The XRD patterns of  $Nb_2O_5$  and supported  $M_2O_3$  (M = Al, Ga, In) samples as synthesized (Fig. 1(a)) show that niobium oxide is amorphous in all samples. Alumina and gallium oxides are well-known for their tendency to poorly crystallize [17]; meanwhile the XRD pattern of the In/Nb sample reveals the presence of well-crystallized indium oxide. The peak intensities and their  $2\theta$  angles have been identified as characteristic of the cubic structure of  $In_2O_3$ . In TG-DSC measurements of niobium oxide, a sharp exothermic peak centered at 817 K without mass loss was observed, indicating a phase transition, assigned to crystallization of  $Nb_2O_5$  [18]. The XRD spectra of niobia after TG-DSC experiment (Fig. 1(b)) showed a well-crystallized hexagonal  $Nb_2O_5$ . Due to crystallization, the BET surface

Table 1

Physico-chemical characteristics of niobia and group III oxides supported on niobia (M = Al, Ga, In)

Sample	Surface ( $\text{m}^2 \text{g}^{-1}$ )	AES-ICP		Theoretic	M/Nb, AES-ICP	M/Nb, XPS
		M (wt%)	$M_2O_3$ (wt%)	$M_2O_3$ (wt%)		
$Nb_2O_5$	108	—	—	—	—	—
Al/Nb	122	6.3	12.0	12.9	0.35	1.7
Ga/Nb	69	14.4	19.3	20.2	0.34	0.9
In/Nb	71	18.3	22.1	23.7	0.27	0.4

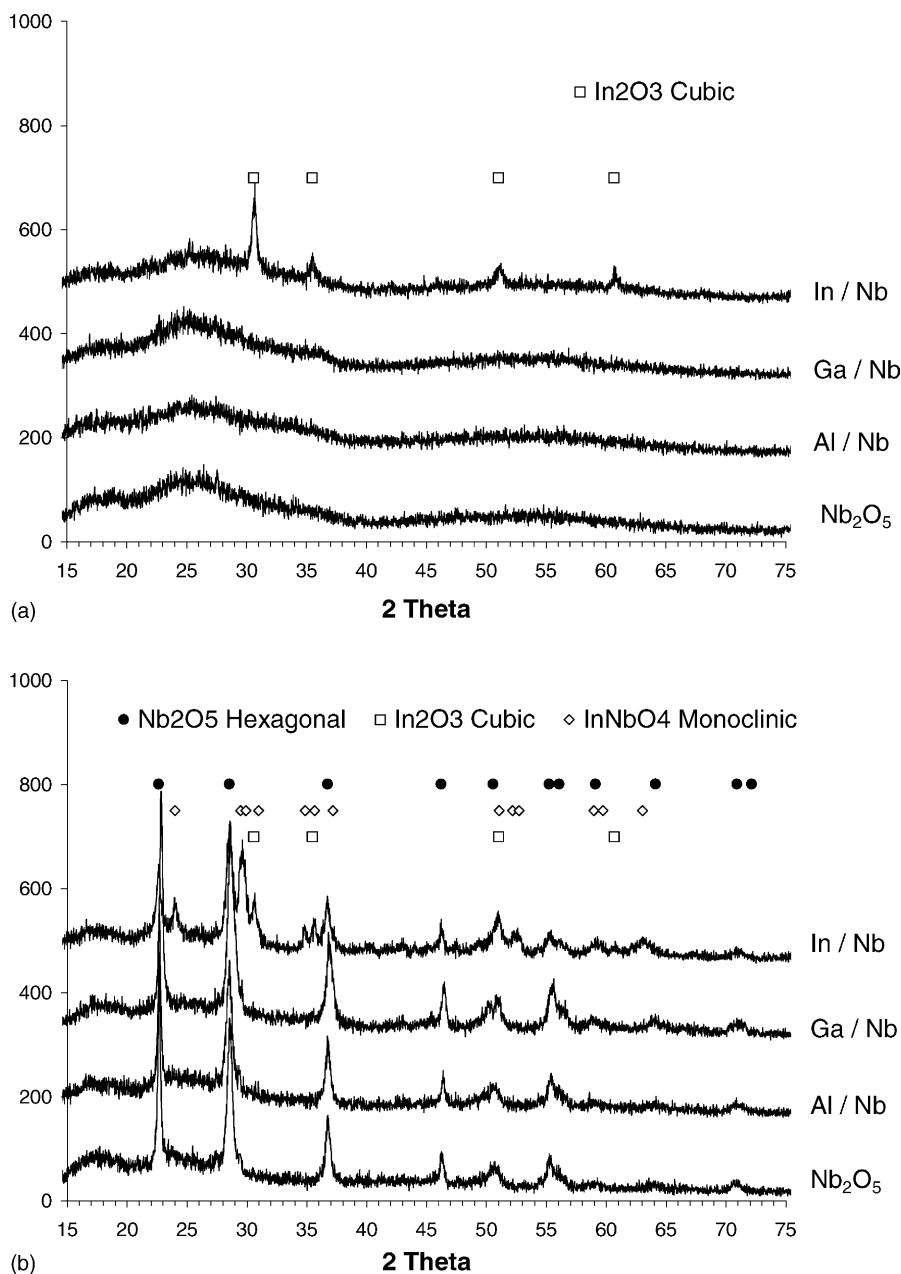


Fig. 1. XRD patterns for niobia supported samples: (a) synthesized catalysts; (b) after TG-DSC measurements.

area strongly decreased to  $41 \text{ m}^2 \text{ g}^{-1}$ . The TG-DSC experiments performed on In/Nb revealed no peak at 817 K, but a wide peak with outset at 873 K and not completely developed at 923 K was observed. The XRD spectra of the In/Nb sample after TG-DSC

(Fig. 1(b)) show the peaks corresponding to crystallized  $\text{Nb}_2\text{O}_5$  and  $\text{In}_2\text{O}_3$ , as well as new peaks that can be attributed to  $\text{InNbO}_4$ . The ability of niobia to form mixed oxides is well-known [2,19,20]. The wide peak observed in the TG-DSC experiment is probably

due to the slow solid–solid reaction leading to the formation of  $\text{InNbO}_4$ . The presence of the peaks corresponding to indium oxide indicates that the reaction is not complete. Like in the case of niobium oxide, after TG-DSC experiment the surface area of the sample decreased to  $33 \text{ m}^2 \text{ g}^{-1}$ . For Ga/Nb and Al/Nb no peak was observed in TG-DSC experiments, nevertheless the crystallization of niobium oxide took place (Fig. 1(b)). The XRD spectra of Ga/Nb and

Al/Nb do not indicate the presence of mixed oxides; other authors have shown that the formation of these mixed (double) oxides occurs at temperatures higher than those used in our experiments (1023 K) [19].

The acidity of the catalysts has been studied by means of microcalorimetry of ammonia adsorption. The operating temperature is important in adsorption experiments. It should be high enough in order to measure the real distribution of the acid site strengths

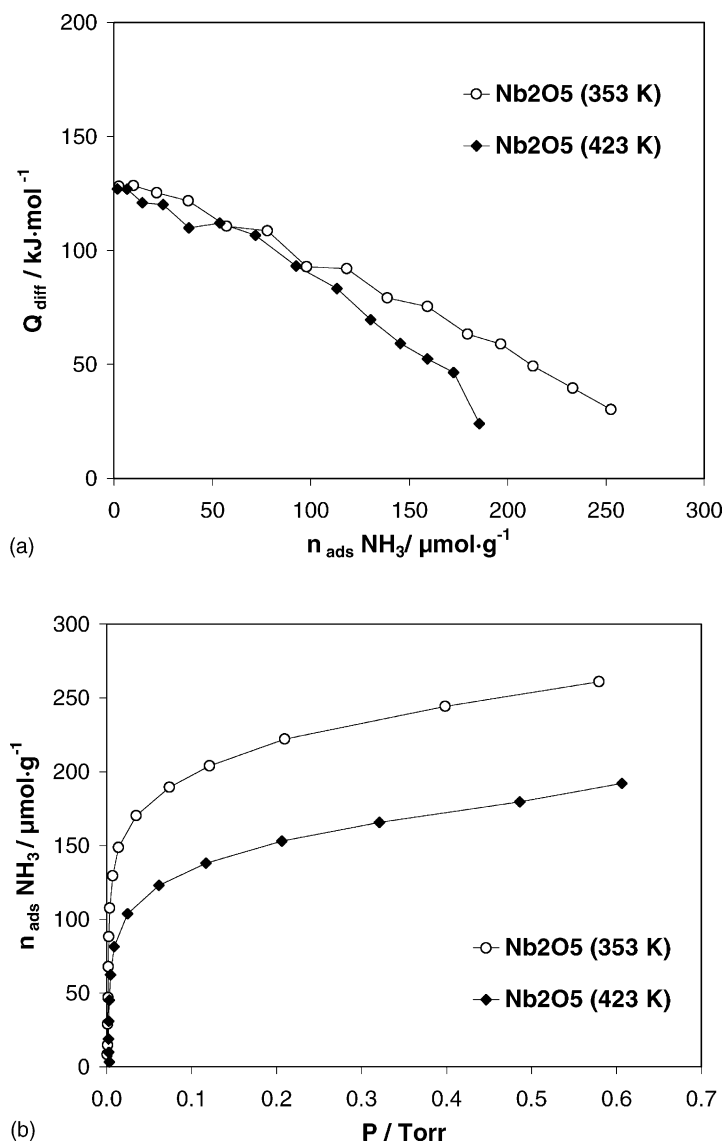


Fig. 2. Ammonia adsorption on niobium oxide at 353 and 423 K: (a) differential adsorption heats; (b) adsorption isotherms.

rather than the accessibility of the sites, and low enough to titrate all the acidic centers. Experiments at two temperatures, 353 and 423 K, have been carried out on niobium oxide samples to establish the best conditions of adsorption. Fig. 2 represents the differential heats: (a) and the isotherms (b) of adsorption of ammonia at both temperatures. Comparing the curves of adsorption heats for Nb<sub>2</sub>O<sub>5</sub> measured at both temperatures, no differences are found in the first part of the curves corresponding to the strongest acidic sites, which means that 353 K is enough to have a real representation of the strength distribution of the acid centers. By contrast, at the higher temperature the adsorption equilibrium on the weaker centers is displaced towards desorption and the total adsorbed amount is smaller (Fig. 2(b)). This justifies the choice of 353 K as operating temperature for the measurements.

The  $V_T$  and  $V_{irr}$  adsorbed volumes are summarized for all the samples in Table 2. Fig. 3(a) represents the differential heats of ammonia adsorption for all samples, while Fig. 3(b) shows the adsorption isotherms. The differential adsorption heats of Al/Nb and Nb<sub>2</sub>O<sub>5</sub> are almost identical except for the first part of the curve where the Al/Nb sample presents a range of higher adsorption heats ( $\approx 42 \mu\text{mol g}^{-1}$ ). This could be attributed to adsorption on newly created alumina acid sites. In our experience [22], alumina presents Lewis acid sites stronger than the acid sites found in the niobia used as support. On the other hand, some authors have suggested that the introduction of an oxide AO<sub>x</sub> onto another oxide BO<sub>y</sub> can generate acid sites [21]. In these models, acidic centers are generated by the charge imbalance along M–O–N linkages.

In Fig. 3(b) it can be seen that the amount of ammonia adsorbed by the Al/Nb sample is larger than for niobia, the difference being more important at higher pressures where the adsorption is due mainly to ph-

ysisorption. Considering that the surface area of Al/Nb is larger than that of Nb<sub>2</sub>O<sub>5</sub> this behavior can be expected. By contrast, the chemisorbed amounts are identical for both samples, indicating that the acidic properties of the two samples are very similar, as already shown by the adsorption heat curves.

The Ga/Nb and In/Nb samples present differential heat curves clearly different from that of niobia. As in the case of Al/Nb, up to a certain adsorbed amount ( $\approx 24 \mu\text{mol g}^{-1}$ ) both samples present adsorption heats higher than on niobia, attributed to the adsorption on newly created centers of guest oxide; subsequently, the adsorption heats become lower than for the bare support. This means that gallium and indium oxide are preferentially deposited on the acid sites of niobia. The more important contribution of the bare support to total acidity (strength and adsorbed amount) for In/Nb than for Ga/Nb is due to the lower dispersion of the first sample, as shown by the XPS measurements.

Fig. 3(b) and Table 2 indicate that the adsorbed ammonia amounts are lower for Ga/Nb and In/Nb. The lower surface areas of both samples in comparison to the support explain the smaller values of total and irreversible adsorbed amounts.

The strength distribution of acid sites is represented in Fig. 4. Arbitrary intervals of adsorption heats have been chosen, which can be considered as representative of strong ( $200 > Q > 150 \text{ kJ mol}^{-1}$ ), medium-strong ( $150 > Q > 100 \text{ kJ mol}^{-1}$ ), medium-weak ( $100 > Q > 50 \text{ kJ mol}^{-1}$ ) and weak ( $50 > Q > 0 \text{ kJ mol}^{-1}$ ) sites. Strong acid sites are present only in supported M<sub>2</sub>O<sub>3</sub> samples, with a greater contribution in the case of the Al/Nb sample, as it has been already shown. The greater part of the acidic sites in Nb<sub>2</sub>O<sub>5</sub> can be considered as having medium strength, while the sites with a low acid strength are less numerous. Al/Nb presents a similar behavior, contrarily to Ga/Nb and In/Nb which display very regular acid site strength distributions.

Basicity has been determined by calorimetry, using SO<sub>2</sub> as probe molecule. The differential heats of SO<sub>2</sub> adsorption on supported group III oxide samples are represented in Fig. 5. Notable differences are found between the three samples, that cannot be explained only by the differences in surface areas. Since no basicity could be observed for Nb<sub>2</sub>O<sub>5</sub>, the basicity should be due to the supported M<sub>2</sub>O<sub>3</sub> oxide. The amphoteric characters of alumina and gallia are well-known, and

Table 2

Total and irreversible adsorbed amounts of ammonia and SO<sub>2</sub>

Sample	NH <sub>3</sub> ( $\mu\text{mol g}^{-1}$ )		SO <sub>2</sub> ( $\mu\text{mol g}^{-1}$ )	
	$V_T$	$V_{irr}$	$V_T$	$V_{irr}$
Nb <sub>2</sub> O <sub>5</sub> (353 K)	220	123	–	–
Nb <sub>2</sub> O <sub>5</sub> (423 K)	152	84	–	–
Al/Nb (353 K)	240	124	68	42
Ga/Nb (353 K)	161	87	28	14
In/Nb (353 K)	181	97	26	10

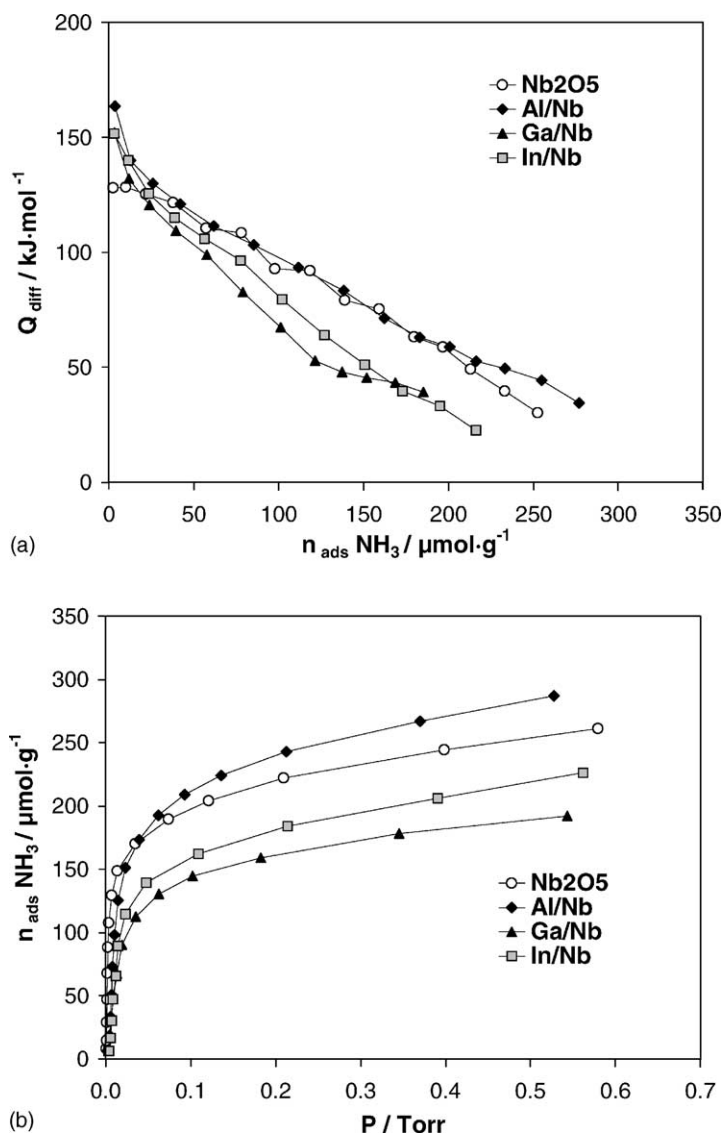


Fig. 3. Ammonia adsorption on Nb<sub>2</sub>O<sub>5</sub>, Al/Nb, Ga/Nb and In/Nb at 353 K: (a) differential adsorption heats; (b) adsorption isotherms.

it is commonly accepted that indium oxide is the most basic of the three group III oxides. However the dispersion of indium oxide in our sample is so low that the adsorbed amount of SO<sub>2</sub> is affected. The same type of behavior is observed for the basicity of the Ga/Nb sample. By contrast, Al/Nb is the sample which presents the largest adsorbed amount of SO<sub>2</sub> and the strongest basic centers. The irreversible adsorbed amounts (see Table 2) are in the order Al/Nb > Ga/Nb > In/Nb.

This order is more related to the dispersion than to the basicity of the guest oxide.

It is worth noting that the total and irreversible SO<sub>2</sub> adsorbed amounts are markedly smaller than the corresponding ammonia amounts, indicating that the surfaces of all the samples can be considered as mostly acidic. The propane conversion and the selectivity towards propene in the non-oxidative dehydrogenation of propane are reported in Fig. 6.

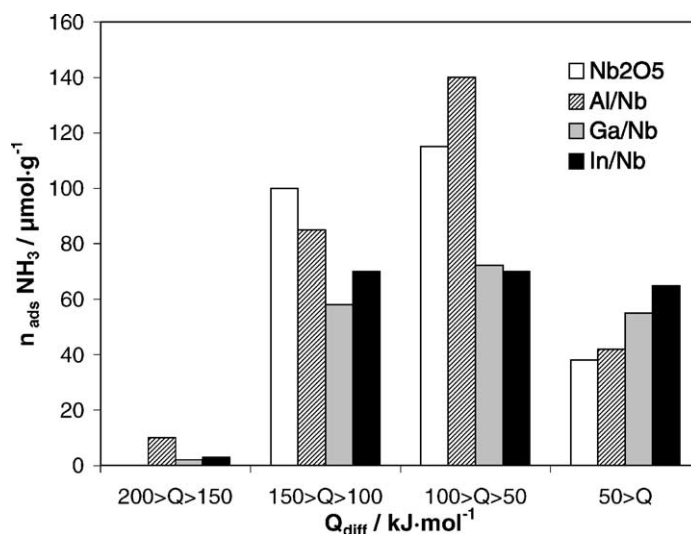


Fig. 4. Acid strength distribution as determined by ammonia adsorption on Nb<sub>2</sub>O<sub>5</sub>, Al/Nb, Ga/Nb and In/Nb.

It is well-known that the non-oxidative dehydrogenation of light alkanes is favored by high temperatures and low pressures. Even if the important decrease of surface areas of the samples at the reaction temperatures, due to niobia crystallization as described above, led to disappearance of some active sites, the temperature improved the reaction kinetics increasing the turnover frequency of the active sites.

On the bare support, the conversion of propane increased with the temperature, reaching a maximum of 3.5% at 873 K; the selectivity towards propene decreased with temperature, reaching 70% at 873 K. Similar trends and values were observed for the Al/Nb sample. In/Nb presents a higher propane conversion, with a maximum of 6.7% reached at 873 K, but the selectivity towards propene was lower (53%) with

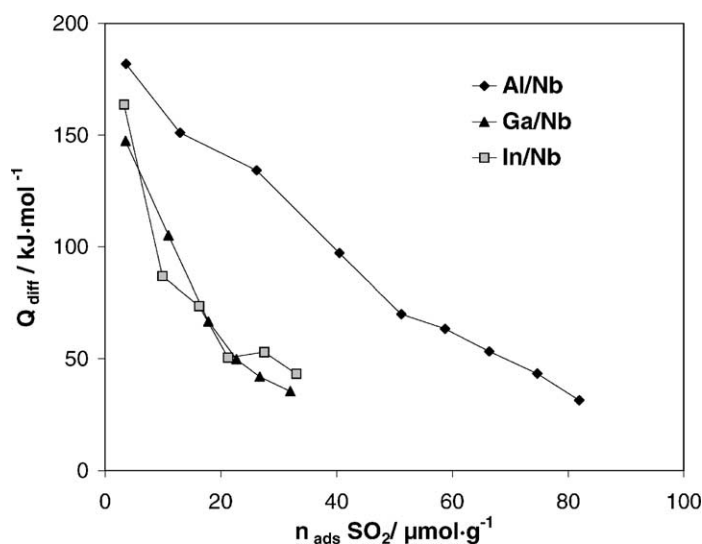


Fig. 5. Differential heats of SO<sub>2</sub> adsorption at 353 K on Nb<sub>2</sub>O<sub>5</sub>, Al/Nb, Ga/Nb and In/Nb.



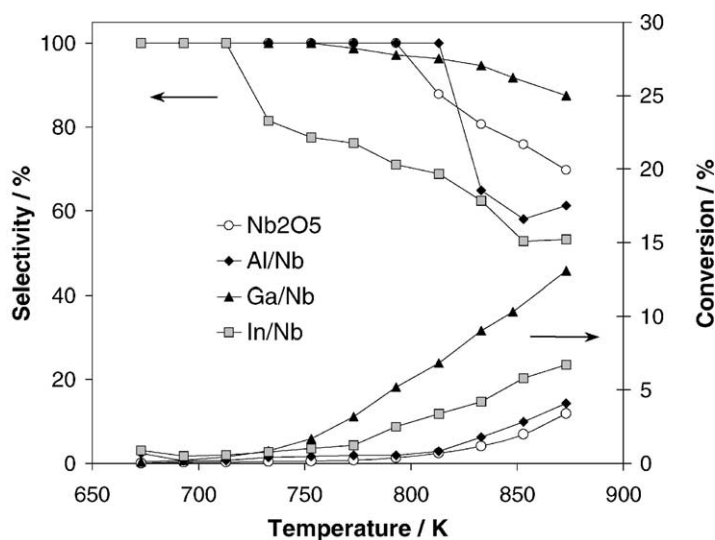


Fig. 6. Conversion of propane and selectivity towards propene as functions of reaction temperature.

values that began to decrease at a lower temperature, around 723 K. Clearly Ga/Nb is the sample that presents the best conversion (13%) and selectivity (88%) of the four studied catalysts. Due to Nb<sub>2</sub>O<sub>5</sub> crystallization, sintering of the supported Al-, In-, and Ga-oxides is expected to occur. Therefore, the order of activity does not reflect the surface extent

of the supported oxides but their intrinsic ability of dehydrogenation towards propane.

Fig. 7 reports the initial rates of propene formation at three different reaction temperatures on niobia and group III oxides supported on niobia. The superior catalytic performance of gallium oxide supported on niobia towards dehydrogenation of propane (in terms

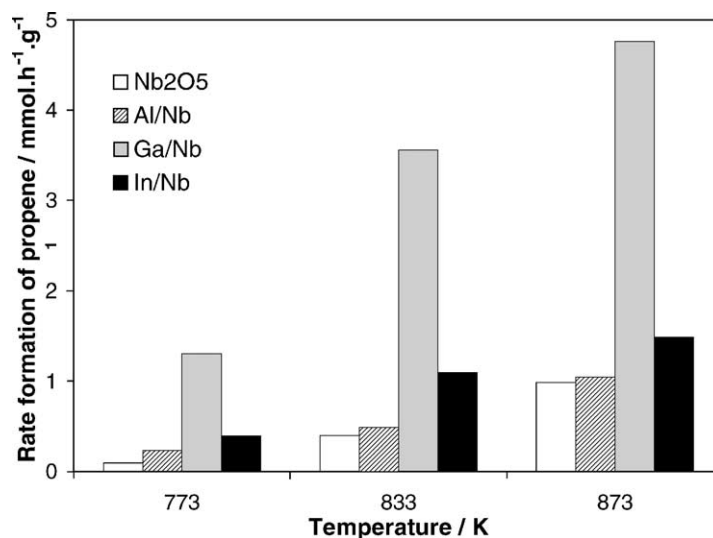


Fig. 7. Initial rate of propene formation vs. reaction temperature in non-oxidative dehydrogenation of propane.

of rate of propene formation or propene yield) is again obvious. If at 773 and 833 K In/Nb shows a higher rate of  $C_3H_6$  formation than the bare support and Al/Nb at 873 K these differences are less important. The XRD patterns of the In/Nb sample after the catalytic test are similar to the spectra recorded after TG-DSC measurements (Fig. 1(b)) showing the formation of a mixed oxide ( $InNbO_4$ ). So, we can conjecture that the formation of mixed oxide negatively influences the increase with temperature of the rate of propene formation.

#### 4. Conclusion

No direct and simple relation could be established between acid/base properties and dehydrogenation function of the samples, even if the measured propane conversions varied in the order  $Ga/Nb > In/Nb > Al/Nb \approx Nb_2O_5$ , exactly the inverse of the order observed in the acidity measurements. In fact, it seems that the ratio of acidic to basic sites is the main criteria which determine the reactivity of the samples. Also, the quality of the dispersion of the guest group III oxide as well as the formation of mixed (double) oxide can strongly influence the catalytic activity in non-oxidative dehydrogenation of propane.

#### Acknowledgements

The authors sincerely thank Dr. Claude Guimon from Université de Pau for fruitful discussions and XPS measurements and M. Dufaux (IRC) for catalytic test.

#### References

- [1] K. Tanabe, S. Okazaki, *Appl. Catal. A* 133 (1995) 191.
- [2] J.C. Vedrine, G. Coudurier, A. Ouqour, P.G. Pries de Oliveira, J.C. Volta, *Catal. Today* 28 (1996) 3.
- [3] T. Uchijima, *Catal. Today* 28 (1996) 105.
- [4] C.L. Tavares da Silva, V.L. Loyola Camorim, J.L. Zotin, M.L. Rocco Duarte Pereira, A. da Costa Faro Jr., *Catal. Today* 57 (2000) 209.
- [5] J. Datka, A.M. Turek, J.M. Jehng, I.E. Wachs, *J. Catal.* 135 (1992) 186.
- [6] A.M. Turek, I.E. Wachs, E. DeCanio, *J. Phys. Chem.* 96 (1992) 5000.
- [7] J.-M. Jehng, I.E. Wachs, *Catal. Today* 16 (1993) 417.
- [8] R. Pohle, M. Fleischer, H. Meixner, *Sens. Actuators B* 68 (2000) 151.
- [9] M. Kudo, T. Kosaka, Y. Takahashi, H. Kokusen, N. Sotani, S. Hasegawa, *Sens. Actuators B* 69 (2000) 10.
- [10] T. Maunula, Y. Kintaichi, M. Inaba, M. Haneda, K. Sato, H. Hamada, *Appl. Catal. A* 15 (1998) 291.
- [11] K. Shimizu, A. Satsuma, T. Hattori, *Appl. Catal. B* 16 (1998) 319.
- [12] K. Nakagawa, C. Kajita, Y. Ide, M. Okamura, S. Kato, H. Kasuya, N. Ikenaga, T. Kobayashi, T. Suzuki, *Catal. Lett.* 64 (2000) 215.
- [13] J. Halász, Z. Kónya, Á. Fudala, A. Béres, I. Kiricsi, *Catal. Today* 31 (1996) 293.
- [14] R.H.H. Smits, K. Seshan, J.R.H. Ross, *J. Chem. Soc., Chem. Commun.* (1991) 558.
- [15] J.R.H. Ross, R.H.H. Smits, K. Seshan, *Catal. Today* 16 (1993) 503.
- [16] W.B. Innes, *Catalysis*, in: P.H. Emmett (Ed.), *Fundamental Principles (Part 1)*, vol. I, Reinhold, New York, Chapter 6, 1954, p. 258.
- [17] B.C. Lippens, J.J. Steggerda, in: B.G. Linsen (Ed.), *Physical and Chemical Aspects of Adsorbents and Catalysts*, Academic Press, New York, Chapter 4, 1970, p. 171.
- [18] T. Ushikubo, *Catal. Today* 57 (2000) 331.
- [19] H. Kominami, M. Inoue, T. Inui, *Catal. Today* 16 (1993) 309.
- [20] Z. Zou, J. Ye, H. Arakawa, *Chem. Phys. Lett.* 332 (2000) 271.
- [21] S.M. Maurer, D. Ng, E.I. Ko, *Catal. Today* 16 (1993) 319.
- [22] A. Auroux, A. Gervasini, *J. Phys. Chem.* 94 (1990) 6371.